

Time-Frequency Spread OFDM/FHMA

¹Kiyoshi Hamaguchi and ²Lajos Hanzo

¹Communications Research Laboratory, ²Dept. of ECS, University of Southampton

¹Yokosuka, 239-0847, Japan, ²Southampton, SO17 1BJ, U.K.

E-mail: ¹hamaguti@crl.go.jp, ²lh@ecs.soton.ac.uk

Abstract- A combined scheme based on Orthogonal Frequency-Division Multiplexing and Frequency-Hopped Multiple Access (OFDM/FHMA) is proposed, in which the transmitted data is spread over both the time and frequency axes without expanding the bandwidth. The OFDM system advocated employs the Walsh-Hadamard Transform (WHT) for spreading the data in the frequency domain and weights the received signal by the estimated Signal-to-Interference Ratio (SIR) for the sake of reducing the effects of interference. The performance recorded, when communicating over an interference-limited channel suggests that the achievable BER improvement is as much as an order of magnitude in comparison to that of an OFDM/FHMA scheme dispending with WHT.

I. Introduction

There are two well-known spread-spectrum multiple-access systems, namely direct-sequence multiple access [1] and frequency-hopped multiple access (FHMA) [1]. In response to the soaring demand for higher quality as well as higher capacity communications, in recent years direct-sequence multiple access has been attracting considerable attention owing to its superior performance. By contrast, there has been a lack of research exploring the benefits of the family of FHMA techniques [2], despite its attractive property that in the context of FH schemes both the frequency- and time-diversity effects may be exploited by using information-spreading over the frequency- and time-domain. The design of FH sequences dedicated to each user is an important issue [3], because the FH sequence determines the number of received signal collisions encountered in each of the FH slots. On the other hand, a combined FH and Forward-Error-Correction (FEC) scheme [4,5] is a strong contender for improving the achievable Bit-Error-Rate (BER) performance. However, FEC schemes usually require an expanded bandwidth, unless coded modulation is employed. In recent years, Orthogonal Frequency Division Multiplex (OFDM) techniques [6,7,8] have also found favour in numerous applications, such as mobile and indoor wireless systems owing to their high spectral efficiency. However, the OFDM signal is sensitive to Co-Channel Interference (CCI) and hence OFDM schemes have to be combined with techniques capable of mitigating the effects of CCI.

In light of the above mentioned circumstances, this study examines an OFDM/FHMA system, in which the transmitted data is spread over both the time and frequency domains without expanding the bandwidth. In the proposed OFDM/FHMA system, Walsh-Hadamard Transform (WHT) [1,7,8] based spreading is employed and the received signal is weighted by the Signal-to-Interference Ratio (SIR) for the sake of reducing the effects of interference. Moreover, in order to determine the dependence of the BER performance on the FH pattern, Einarsson's hopping sequence assignment scheme [3]

was involved. We will show that when transmitting over an interference-limited channel, the achievable BER performance may be improved by as much as an order of magnitude in comparison to that of the OFDM/FHMA scheme dispending with WHT-based spreading.

II. Concept of the Proposed System

Fig. 1 characterizes the concept of the proposed system. At the transmitter, the binary data sequence is converted to the LN symbols of an arbitrary modulation scheme such as Quadrature Amplitude Modulation (QAM), which is shown as a block labeled ' LN QAM symbols' in the figure. Next, a block of LN QAM symbols is transformed by using the WHT, where each input symbol influences each output symbol, effectively spreading the influence of each QAM symbol. The transformed data block representing LN QAM symbols is mapped to a total of L FH slots, and each of these L slots carries N number of WHT-spread symbols. These WHT-spread symbols are then mapped to OFDM symbols. Specifically, H number of OFDM symbols each constituted by J subcarriers are generated, which also incorporate frequency-domain pilot- and null-symbols used for estimating the SIR-levels encountered, as it will be outlined below [4].

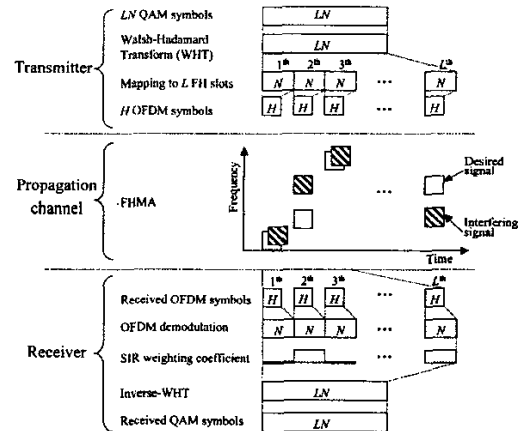


Fig. 1 Concept of the proposed system.

It is assumed in Fig. 1 that slots 1 and 3 are affected by the interference imposed by other users in the propagation channel. The power of these signals depends on their propagation environments, such as the distance-dependent path loss, the shadowing effects, and the signal blocking caused by obstacles between the desired and undesired users. Moreover, the received signal may be affected by dispersion, when communicating over frequency-selective fading environments.

The received signal is demodulated by the OFDM demodulator. Following OFDM demodulation but before the subcarrier decision stage, the received signal of each subcarrier is scaled using a weighting scheme, which deweights the subcarriers suffering from a low Signal-to-Interference Ratio (SIR) at the receiver stage labeled 'SIR weighting coefficient' in Fig. 1. Finally, the desired signal associated with each of the L FH slots is recovered by using the Inverse WHT (IWHT) and the QAM demodulator. As a benefit of the operations of spreading and despreading using the WHT and IWHT combined with the SIR weighting scheme, the adverse effects of low-SIR subcarriers on the averaged BER performance is potentially improved. Suffice to say here that the SIR-level is estimated with the aid of the null-symbols used for SIR-estimation, which are periodically inserted into the spectrum of the desired signal during each FH slot at the transmitter, and the corresponding interference-contaminated received signal levels are recorded at the receiver. In other words, since the transmitted signal of the corresponding OFDM subcarrier is known to be zero, the received energy is a direct consequence of CCI. Having determined the level of CCI interference, the desired signal's level is determined with the aid of the frequency-domain channel sounding pilots embedded into the OFDM signal's spectrum.

III. System Model Description

A. Transmitter

The upper part of Fig. 2 shows the block diagram of the transmitter, which consists of the QAM modulator, the WHT, serial-to-parallel (S/P) and parallel-to-serial (P/S) converters, the OFDM modulator and the frequency-hopping stage. In order to simplify our discourse, the standard operation of inserting and that of extracting the cyclic extension is not discussed further. The duration of this cyclic extension has to be longer than that of the channel-induced dispersion for the sake of efficiently mitigating the multi-path fading. Furthermore, the inclusion of the cyclic prefix mitigates the effects of imperfect FH slot synchronization.

Recall from Fig. 1 that the model assumes that an N -bit data block is transmitted over $L=2^l$ ($l=1,2,\dots$) FH slots, each slot hosting H OFDM symbols having J subcarriers per symbol. Without loss of generality, we assume $H=1$. It is also assumed that $\mathbf{D}^{(T)}=(d_0, d_1, \dots, d_{N-1})$ is a binary transmitted data block of user k , which is converted to m -ary QAM symbols at the QAM modulator block of Fig. 2. Then the M -symbol QAM block is given by $\mathbf{A}^{(T)}=(a_0^{(T)}, a_1^{(T)}, \dots, a_{M-1}^{(T)})$, where we have $M=N/\log_2(m)$ when m -ary QAM is applied. Then the QAM symbol block $\mathbf{A}^{(T)}$ is transformed using the WHT for the sake of

generating the M -component signal vector $\mathbf{B}^{(T)}$ as

$$\mathbf{B}^{(T)} = \text{WHT}(\mathbf{A}^{(T)}), \quad (1)$$

where $\text{WHT}(\cdot)$ denotes the Walsh-Hadamard transformation. The resultant M -symbol vector $\mathbf{B}^{(T)}$ is mapped to L parallel streams by the S/P block of Fig. 2, each of which will be mapped to one of the L number of FH slots. Hence the output of the WHT block is partitioned according to $\mathbf{B}^{(T)}=(\mathbf{b}_0^{(T)}, \mathbf{b}_1^{(T)}, \dots, \mathbf{b}_{L-1}^{(T)})$, and the resultant M/L -component subvectors $\mathbf{b}_l^{(T)}=(b_{l,0}^{(T)}, b_{l,1}^{(T)}, \dots, b_{l,M/L-1}^{(T)})$ as well as the Nn number of SIR-estimation null-symbols [4], Np pilot-symbols used for frequency-domain channel transfer function estimation and the $J-(M/L+Nn+Np)$ number of padding symbols used for insuring that the block-length becomes an integer power of 2, before the IFFT-based modulation is invoked, are mapped to a J -subcarrier OFDM symbol, as seen in Fig. 2.

It is assumed furthermore that $\mathbf{F}_k=(f_{k,0}, f_{k,1}, \dots, f_{k,L-1})$ is a hopping frequency set, where $f_{k,l}$ is the frequency of user k during the l -th FH slot. The k -th user's modulated signal at the n -th sample of the OFDM symbol during the l -th FH slot can be expressed as

$$s_k(n, l) = \frac{1}{J} e^{j2\pi f_{k,l} n \Delta_t} \sum_{m=0}^{J-1} b^{(T)}_{l,m} e^{j2\pi m n \Delta_t / T_s}, \quad \text{for } 0 \leq n \Delta_t < T_s, \quad (2)$$

where T_s and Δ_t are the time-domain OFDM symbol duration and the sampling interval duration, respectively, having a relation of $T_s = J \Delta_t$. We note furthermore that $b^{(T)}_{l,m}$ in Equation (2) consists of $b^{(T)}_{l,m}$, null-symbols and pilot-symbols and we have $b^{(T)}_{l,m} = 0$ for $m \geq M/L + Nn + Np$, which are the padding symbols. These null- and pilot symbols are inserted into the modulating signal stream $b^{(T)}_{l,m}$ at the output of the WHT block at predetermined positions, as seen in Fig. 2.

B. Channel and Receiver

The received signal suffers from both channel impairments and CCI imposed by other users activating the same FH frequency within a given time slot. We note that the signal strength is expected to vary on a slot-by-slot basis. It is also assumed that the received signal suffers from frequency-selective fading, which is characterized by the complex-valued dispersive Channel Impulse Response (CIR) $h_k(l, n)$. Fine frequency-, frame-, and symbol-synchronization

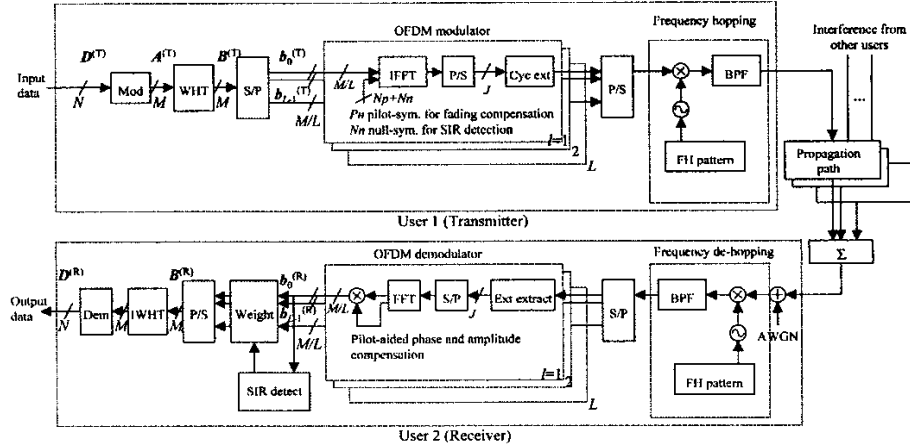


Fig. 2 Block diagram of the proposed system.

are assumed to have been accomplished. The sampled signal at the receiver's input can be expressed as

$$r_k(l, n) = h_k(l, n) \otimes s_k(l, n) + \sum_{u=0, u \neq k}^K I_u(l, n) + n_u(l, n), \quad (3)$$

where the second and third terms on the right of Equation (3) represent the sum of the interference imposed by the interfering users and the receiver's thermal noise, respectively, while the symbol \otimes denotes convolution.

The bottom part of Fig. 2 portrays the block diagram of the receiver, which essentially consists of the frequency de-hopper, S/P and P/S converters, the OFDM demodulator, the null-symbol assisted SIR detector and weighting based combining stages, the IWHT and QAM de-mapping functions. These blocks essentially constitute the inverse of the operations involved at the transmitter, while the weighting based combining stage of the receiver will be discussed in Section IV.

By using the vector notation of $\mathbf{R}_k = (r_k(l, 0), r_k(l, 1), \dots, r_k(l, J))$, the demodulated OFDM signal $\mathbf{b}^{(R)_i}$ at the output of the FFT based OFDM demodulator can be expressed as

$$\mathbf{b}^{(R)_i} = FFT(\mathbf{R}_{k,i}). \quad (4)$$

After the null- and pilot-symbols as well as the padding symbols are extracted from the received symbol stream $\mathbf{b}^{(R)_i}$, pilot-aided phase- and amplitude compensation is performed at the OFDM demodulator [6], which results in the vector $\mathbf{b}_i^{(R)} = (b_{i,0}^{(R)}, b_{i,1}^{(R)}, \dots, b_{i,M/L}^{(R)})$. The corresponding signal is then weighted by the null-symbol based SIR estimates, resulting in the signal $\mathbf{B}^{(R)} = (\mathbf{b}_0^{(R)}, \mathbf{b}_1^{(R)}, \dots, \mathbf{b}_{L-1}^{(R)})$, as seen in Fig. 2. More precisely, the SIR-based received signal weighting exploits the interference estimates derived using the null-symbols and the signal-power estimates based on the frequency-domain pilots, as described in Section IV. Following despreading using the IWHT as well as QAM symbol decisions in the 'IWHT' and 'Dem' blocks of Fig. 2, respectively, the resultant N -component binary data $\mathbf{D}^{(R)}$ is given by

$$\mathbf{D}^{(R)} = Dec(IWHT(\mathbf{B}^{(R)})) \\ = Dec(IWHT(\lambda \mathbf{B}^{(T)} + \sum_{k=0, k \neq i}^K I'_k + n'_k)), \quad (5)$$

where I'_k and n'_k are the interference and noise components, respectively, after OFDM demodulation, while λ is a coefficient dependent on the reliability of the OFDM demodulation process. More explicitly, when perfect frequency-domain pilot-aided phase- and amplitude compensation is performed by the OFDM demodulator, we have $\mathbf{A}^{(T)} = IWHT(\lambda \mathbf{B}^{(T)})$. Again, $Dec(\cdot)$ denotes the QAM symbol decision operator of the corresponding modulation scheme. Equation (5) suggests that the interference-induced contamination is spread during the IWHT process and the effects of interference are thus more uniformly spread during the decision process, potentially holding the promise of error-free data recovery, which would have been less likely without 'smearing' or averaging the effects of interference. Viewing this phenomenon from a different perspective, a high instantaneous interference peak may obliterate a chip of the Walsh-Hadamard spreading code, but this may still allow the error-free recovery of the code itself. Therefore we can expect

a BER improvement, when we use a combination of frequency-hopping and WHT based spreading.

IV. SIR-Weighted Combining

For the sake of mitigating the effects of CCI during the symbol decisions, the scaled vector $\mathbf{B}^{(R)} = \{\rho_0 \mathbf{b}_0^{(R)}, \rho_1 \mathbf{b}_1^{(R)}, \dots, \rho_{L-1} \mathbf{b}_{L-1}^{(R)}\}$ is used for replacing $\mathbf{B}^{(R)} = (\mathbf{b}_0^{(R)}, \mathbf{b}_1^{(R)}, \dots, \mathbf{b}_{L-1}^{(R)})$ in Equation (5) and in Fig. 2, where the multiplier ρ_i , $0 \leq \rho_i \leq 1$, is a function of the CCI strength experienced during the i -th slot. In order to detect the CCI level experienced, known SIR-estimation symbols having a zero amplitude, namely so-called null-symbols are inserted into the spectrum of each OFDM symbol of each FH slot. The CCI level experienced is determined by recording the corresponding received signal level, while the desired signal level is estimated on the basis of the received frequency-domain pilot symbols¹.

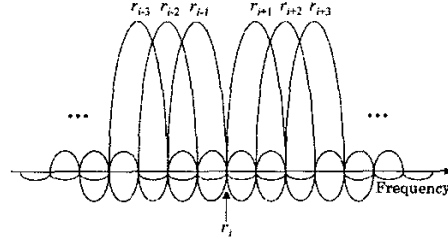


Fig. 3 Stylised illustration of the interference detection scheme.

Fig. 3 augments the concept of the SIR detection scheme. As shown in the figure, when encountering an Additive White Gaussian Noise (AWGN) channel and assuming perfect OFDM demodulation at the receiver, the received signal level, r_i , corresponding to a null symbol in the frequency domain provides us with an indication of the CCI power level. We let the number of subcarrier positions allocated to the pilot symbols and null symbols be $\{n_p\}$ and $\{n_n\}$. The estimated SIR, namely $SIR_{est}(l)$ in the l th FH slot can be expressed as:

$$SIR_{est}(l) = \frac{N_n \sum_{i \in n_p} \|r_i\|^2}{N_p \sum_{i \in n_n} \|r_i\|^2}. \quad (6)$$

The proposed SIR-weighted combining² can be performed by using the reliability measure $SIR_{est}(l)$ for weighting the received signal contributions. For the sake of defining the optimum weighting coefficient $\rho_{opt,l}$ that is capable of minimizing the BER, the OFDM/FHMA system (which selects one of Q frequencies for each FH slot and which suffers from undesired interfering OFDM/FHMA signals also assuming Q frequencies) was determined under three conditions: (i) without WHT/IWHT, (ii) with the aid of WHT/IWHT, (iii)

¹ In practical situations, the pilot symbols are also contaminated by interference. Hence, for performing an accurate estimation, we have to assume a certain minimum SIR level, for example $SIR > 5$ dB.

² We used here the SIR, rather than SINR, since we intend to reduce the effects of interference in the proposed FHMA system.

invoking both WHT/IWHT and the SIR-weighted combining scheme.

The average desired signal power, the sum of the interfering signal power and the receiver's thermal noise power associated with the l -th FH slot are defined as $\sigma_s^2(l)$, $\sigma_i^2(l)$, and σ_n^2 , respectively. The average BER of system (i), namely $BER_{(i)}$, can then be approximated as

$$\varphi_{(i)} = \frac{\sigma_s^2(l)}{\sigma_s^2(l) + \sigma_n^2}, \quad BER_{(i)} = \frac{1}{L} \sum_{l=0}^{L-1} P_e(\varphi_{(i)}), \quad (7)$$

where $P_e(\varphi)$ denotes the theoretical BER [6] associated with the modulation scheme employed at SINR= φ .

In the context of system (ii), the WHT and IWHT operations spread and de-spread the signals over multiple FH slots, hence the corresponding $BER_{(ii)}$ is given by

$$\varphi_{(ii)} = \frac{\sum_{l=0}^{L-1} \sigma_s^2(l)}{\sum_{l=0}^{L-1} \sigma_s^2(l) + L\sigma_n^2}, \quad BER_{(ii)} = P_e(\varphi_{(ii)}). \quad (8)$$

Regarding system (iii), a less than unity SIR-dependent weighting coefficient is invoked for reducing not only the interfering signal's power, but also the desired signal's power. The resultant reduced desired-signal power may lead to mis-classification as an interfering signal. When this apparent interference is considered, $BER_{(iii)}$ is given by

$$\varphi_{(iii)} = \frac{\sum_{l=0}^{L-1} \sigma_s^2(l)}{\sum_{l=0}^{L-1} \{(1-\rho_l)^2 \sigma_s^2(l) + \rho_l^2 \sigma_i^2(l)\} + L\sigma_n^2}, \quad (9a)$$

$$BER_{(iii)} = P_e(\varphi_{(iii)}). \quad (9b)$$

In order to determine $\rho_{opt,l}$ for the sake of attaining the minimum $BER_{(iii)}$ for all $l \in \{0, 1, \dots, L-1\}$, a suitable approach is to minimize Equation (9a) by using standard optimization techniques, namely by evaluating its partial derivatives with respect to the desired weighting coefficients ρ_l , yielding:

$$\frac{\partial \varphi_{(iii)}}{\partial \rho_l} = \frac{\sum_{l=0}^{L-1} 2\sigma_s^2(l) \cdot \{(1-\rho_l)\sigma_s^2(l) - \rho_l\sigma_i^2(l)\}}{\left[\sum_{l=0}^{L-1} \{(1-\rho_l)^2 \sigma_s^2(l) + \rho_l^2 \sigma_i^2(l)\} + L\sigma_n^2 \right]^2}. \quad (10)$$

At the optimum point, the partial derivatives $\partial \varphi_{(iii)} / \partial \rho_l$ become zero for all $l \in \{0, 1, \dots, L-1\}$, yielding the required formula between $\rho_{opt,l}$ and $SIR(l)$ as follows:

$$\rho_{opt,l} = \frac{1}{1 + \frac{\sigma_i^2(l)}{\sigma_s^2(l)}} = \frac{1}{1 + \frac{1}{SIR(l)}}. \quad (11)$$

From Equation (11), we obtain the required coefficients ρ_l by using $SIR_{est}(l)$ in the form of:

$$\rho_l = (1 + SIR_{est}(l)^{-1})^{-1}. \quad (12)$$

Finally, the minimum BER, namely $BER_{(iii),min}$ is obtained by substituting $\rho_{opt,l}$ from Equation (11) into Equation (9a) and (9b), yielding:

$$BER_{(iii),min} = P_e\left(\frac{\sum_{l=0}^{L-1} \sigma_s^2(l)}{\sum_{l=0}^{L-1} \frac{1}{\sigma_s^2(l)^{-1} + \sigma_i^2(l)^{-1}} + L\sigma_n^2}\right). \quad (13)$$

V. Simulation Results and Discussions

The BER performance of the proposed OFDM/FHMA system was evaluated by computer simulation. A random-number generator was used for selecting the random frequency for each FH slot with a uniform probability. It was also assumed that all interfering signals had the same power level, where the SIR was defined as the ratio of desired-signal power to any of the interfering signal powers. An AWGN channel was assumed. It was also assumed that the OFDM/FHMA receiver was capable of maintaining perfect synchronization and perfect frequency-domain amplitude/phase compensation. Three frequency-domain null-symbols and three channel sounding pilot symbol subcarriers were inserted into each FH slot for the sake of maintaining a good balance between accurate SIR and channel transfer function estimation as well as high effective throughput. The simulation conditions are summarized in Table 1.

Fig. 4 shows the BER versus SNR performance of the proposed system, when the number of users supported is one (no CCI), 24 or 48. This figure includes the corresponding BER curves for OFDM/FHMA both without WHT/IWHT based spreading, and those for the proposed system employing WHT/IWHT both with and without SIR-weighted combining. This result was recorded for a SIR of 10 dB, as an example, concerning each interfering signal. It is clear that the BER performance of the system including WHT/IWHT is better than that without WHT/IWHT, and the SIR-weighted combining further improves the achievable BER. This is because the detrimental influence of the low-SIR slots that were gravely affected by the interfering signals is reduced during the SIR-weighted combining process.

Figs. 5 and 6, respectively, portray the BER versus the number of users performance of the proposed system (both with and without frequency hopping) for a SNR of 16 dB. Fig. 5 confirms that the system benefiting from SIR-weighted combining achieves the best performance in conjunction with frequency hopping. As the number of users decreases, the achievable BER performance improves as a benefit of the reduced interference. By contrast, in case of no FH the effects of interference remain more detrimental even when the number of users is reduced, as seen in Fig. 6.

Fig. 7 shows the achievable BER performance under the same conditions as those for Figs. 5 and 6, except that Einarsson's frequency-hopping assignment scheme [3] was used instead of random hopping for the sake of minimizing the probability of FH slot collisions. It is clear that the BER improved slightly, when the number of users was 20 or less. However, for a high number of users the BER performance was similar to that recorded in Fig. 5.

The above results suggest that the achievable BER improvement recorded, when communicating over interference-limited channels may be as high as an order of magnitude, provided that the number of users is around 25 or less. Moreover, the attainable improvement becomes lower,

when the number of users is high in comparison to that, when the OFDM/FHMA system is operating without the WHT/IWHT aided signal spreading scheme.

Table 1 Simulation conditions.

Parameter	Value
Multiple-access scheme	FHMA
Number of FH frequencies	64
Number of FH slots	8
Modulation	Gray-coded QPSK/OFDM
Number of OFDM subcarriers	64
Number of null-symbols	3-symbols/FH slot
Number of pilot-symbols	3-symbols/FH slot
Propagation channel	AWGN channel

VI. Conclusion

An OFDM/FHMA scheme using the WHT and the proposed SIR-weighted combining was developed. In the investigated scenario the achievable BER is as much as an order of magnitude less than that of the OFDM/FHMA benchmark scheme using no WHT-based spreading. Alternatively, the number of users supported may be increased by about a factor of three at $BER=10^{-3}$ with the advent of the proposed system. Our future work will quantify the achievable BER improvements over dispersive fading channels. For a range of related system studies and further research topics the interested reader might like to consult references [1,6,8,9].

Acknowledgment

This work was supported by a grant from the JSPS overseas research fellowship of Japan.

References

- [1] Hanzo L., et al., *Single- and Multicarrier CDMA*, John Wiley-IEEE Press, 2003.
- [2] Peterson R.L., et al., *Introduction to Spread Spectrum Communications*, Prentice Hall, 1995.
- [3] Einarsson G., "Address Assignment for a Time-Frequency-Coded, Spread-Spectrum System," *The Bell System Technical Journal*, Vol. 59, No. 7, pp. 1241-1255, Sep. 1980.
- [4] Hamaguchi K., Moriyama E., Kamio Y., and Sasaoka H., "Transmission Experiments on Slow-FH/16QAM System for Land Mobile Communications," *IEICE Trans. on Communications*, Vol. E81-B, No. 7, pp. 1444-1452, Jul. 1998.
- [5] Hamaguchi K., Kamio Y., Sampei S., and Morinaga N., "Performance of Slow-FH/16-QAM System with Interference-Immunity Decoding and Transmission Power Control for Land Mobile Radio," *Proc. of the IEEE Vehicular Technology Conference*, Vol. 3, pp. 1810-1814, Sep. 1999.
- [6] Hanzo L., et al., *Single- and Multi-Carrier Quadrature Amplitude Modulation*, John Wiley-IEEE Press, 2000.
- [7] Dlugaszewski Z., Wesolowski K, and Lobeira M., "Performance of Several OFDM Transceivers in the Indoor Radio Channels in 17 GHz Band," *Proc. of the IEEE Vehicular Technology Conference*, Vol. 2, pp. 825-829, May 2001.
- [8] Hanzo L., et al., *OFDM and MC-CDMA*, John Wiley-IEEE Press, 2003.
- [9] Hanzo L., et al., *Turbo Coding, Turbo Equalisation and*

Space-Time Coding, John Wiley-IEEE Press, 2002.

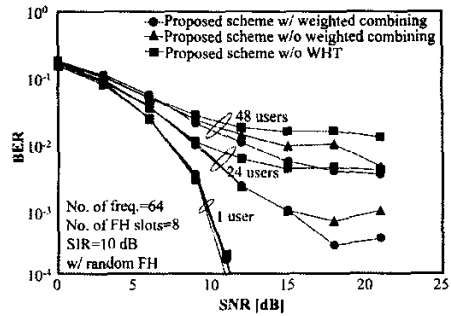


Fig. 4 BER versus SNR performance over the AWGN channel.

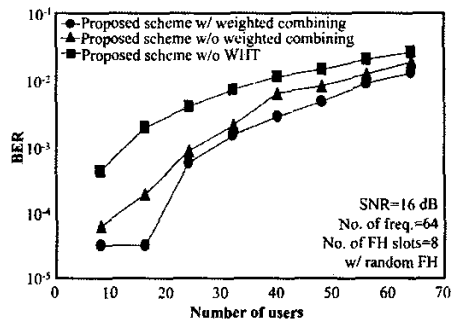


Fig. 5 BER versus the number of users performance using random FH over the AWGN channel.

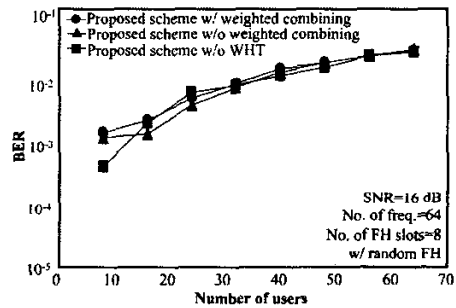


Fig. 6 BER versus the number of users performance without FH over the AWGN channel.

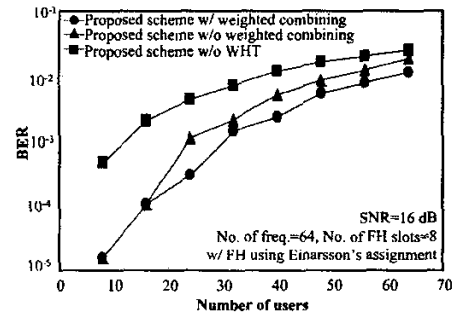


Fig. 7 BER versus the number of users performance using Einarsson's multi-user FH address assignment scheme [3] over the AWGN channel.